

# Electrical power factor for a single crystal tonpiliz versus a plate with matching layers

Røed, Ellen Katrine Sagaas<sup>1, 2</sup>; Bring, Martin<sup>2</sup>; Tichy, Frank<sup>2</sup>; Åsjord, Else-Marie<sup>2</sup>; Hoff, Lars<sup>1</sup>

<sup>1</sup>Department of Microsystems, University of South-Eastern Norway, Horten, Norway

<sup>2</sup>Kongsberg Maritime Sensors and Robotics Horten, Norway

This is an Accepted Manuscript of an article published by IEEE Online in 2021 *IEEE International Ultrasonics Symposium (IUS)* on November 12, 2021, available online:

<https://doi.org/10.1109/IUS52206.2021.9593402>

Røed, E. S., Bring, M., Tichy, F., Åsjord, E. -M., & Hoff, L. (2021, September 11-16). Electrical power factor for a single crystal tonpiliz versus a plate with matching layers [Conference presentation]. *2021 IEEE International Ultrasonics Symposium (IUS)*. Xi'an. <https://doi.org/10.1109/IUS52206.2021.9593402>

**© 2021 IEEE. Personal use of this material is permitted. Permission from IEEE must be obtained for all other uses, in any current or future media, including reprinting/republishing this material for advertising or promotional purposes, creating new collective works, for resale or redistribution to servers or lists, or reuse of any copyrighted component of this work in other works.**

# Electrical power factor for a single crystal tonpiliz versus a plate with matching layers

Ellen Sagaas Røed<sup>\*†</sup>, Martin Bring<sup>\*</sup>, Frank Tichy<sup>\*</sup>, Else-Marie Åsjord<sup>\*</sup> and Lars Hoff<sup>†</sup>

E-mail: ellen.sagaas.roed@km.kongsberg.com, martin.bring@km.kongsberg.com, frank.tichy@km.kongsberg.com, else-marie.asjord@km.kongsberg.com, Lars.Hoff@usn.no

<sup>\*</sup>Sensors and Robotics, Kongsberg Maritime, Horten, Norway

<sup>†</sup>Department of microsystems, University of South-Eastern Norway, Horten, Norway

**Abstract**— For underwater transducers mounted on small platforms, reactive electrical power can constitute a main restriction on the usable frequency range. The frequency range in which the amount of reactive power is acceptable can be increased by increasing the electromechanical coupling coefficient of the active material. However, to avoid large electrical power factor ripple, the transducer design must also have a low mechanical quality factor,  $Q_m$ . A ferroelectric single crystal can have electromechanical coupling coefficient  $k = 0.9$ . The optimum  $Q_m$  is then as low as 0.6, which is challenging to achieve. We investigated this challenge for a tonpiliz design, by calculating  $Q_m$  for different combinations of head masses and tonpiliz stiffnesses, and by calculating the stiffness to density ratio required in the head material to avoid flexural resonances. The effective coupling coefficient of a real transducer is reduced compared to the material coupling coefficient, and in many applications some power factor ripple can be accepted. Both factors relax the  $Q_m$  requirement. We calculated the power factor of a tonpiliz design with  $k = 0.82$  and  $Q_m = 1.9$ , and showed that the power factor ripple is smaller than 0.2 in a frequency band that is 150 % wide relative to the resonance frequency. The frequency independent matching inherent in the tonpiliz gives this design an advantage regarding power factor ripple, and this can weigh up for a large  $Q_m$ . We showed this by comparing the tonpiliz to an air-backed composite plate. Like the tonpiliz, the composite plate had  $k = 0.82$ , but it was matched to water by two conventional acoustic matching layers. Compared to the tonpiliz, the composite design had a larger distance between the  $-3$ dB points of the acoustic power. Beyond these points, the acoustic power was however falling off more rapidly, resulting in an electrical power factor ripple of nearly 0.5.

**Keywords**—single crystal, matching layer, 1-3 composite, tonpiliz

## I. INTRODUCTION

Our ability to monitor marine ecosystems is now being extended by use of small robots. These small robots have room for only a few transducers, requiring each transducer to collect diverse information, and hence to cover a large frequency range. The transducer electronics must be compact and is confined in a small space, and the amount of reactive electrical power can constitute a main restriction on the usable frequency range. Using the lumped Butterworth-van Dyke (BVD) model in Fig. 1. and Stansfield's bandwidth definition [1], Moffett et. al [2] found the maximum frequency band over which a transducer can transmit high power. Referring the bandwidth to the resonance frequency, they found a width of 200 % for electromechanical coupling coefficient  $k = 0.9$  compared to

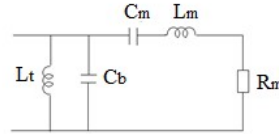


Fig. 1: BVD circuit showing tuning inductance,  $L_t$ , blocked capacitance,  $C_b$ , motional capacitance,  $C_m$ , motional inductance,  $L_m$  and motional resistance,  $R_m$ .

100 % for  $k = 0.7$ . Ferroelectric single crystals can have  $k \geq 0.9$ , and we are investigating whether use of single crystals as the active material can help us make transducers with a large usable frequency band.

## II. OPTIMUM MECHANICAL QUALITY FACTOR

Even if the *maximum obtainable* band is increased by increasing  $k$ , the *achieved* bandwidth for a specific transducer design will depend on the mechanical quality factor,  $Q_m$ , of that design. For the BVD circuit,  $Q_m$  is given by [2]

$$Q_m = \omega_0 \frac{L_m}{R_m} = \frac{1}{\omega_0 C_m R_m} \quad (1)$$

where  $\omega_0$  is the angular resonance frequency,  $L_m$  the motional inductance,  $R_m$  the motional resistance and  $C_m$  the motional capacitance. The power,  $P$ , used to drive a transducer consists of a real part,  $|P| \cos \theta$ , and a reactive part,  $|P| \sin \theta$ , where  $\theta$  is the phase of the transducer's electrical impedance. The power factor can be expressed as [3, p. 70]

$$PF = \cos \theta = 1/\sqrt{1 + \tan^2 \theta} \quad (2)$$

$$\tan \theta = \left[ \frac{1-k^2}{k^2} \frac{1}{Q_m} - Q_m + \frac{1-k^2}{k^2} Q_m \left( \frac{\omega}{\omega_0} - \frac{\omega_0}{\omega} \right)^2 \right] \left( \frac{\omega}{\omega_0} - \frac{\omega_0}{\omega} \right). \quad (3)$$

The above expression for  $\tan \theta$  is valid for a transducer after the clamped capacitance has been tuned out by a parallel inductor, as shown in Fig. 1. The tuned power factor for  $k = 0.9$  and different values of  $Q_m$  is shown in Fig. 2a, revealing that  $Q_m$  must be close to 0.6 for the power factor to be approximately flat between the flanks. The power factor for  $k = 0.7$  is shown in Fig. 2b for comparison.

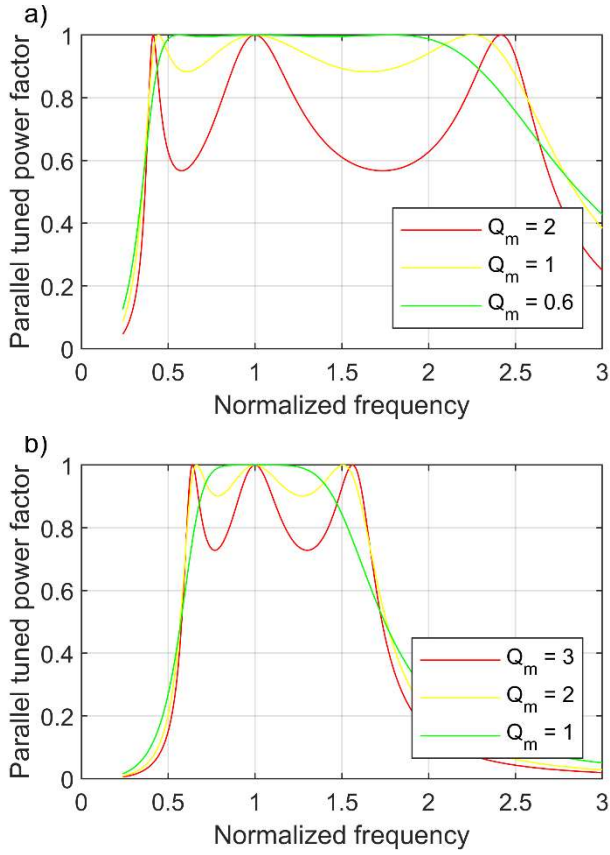


Fig. 2: Parallel tuned electrical power factor for a)  $k = 0.9$  and b)  $k = 0.7$ . The figure corresponds to fig. 2.12 in [3, pp. 72-73].

For most designs, the effective coupling coefficient is reduced compared to the material coupling coefficient. When the effective  $k$  is reduced to 0.82, the optimum  $Q_m$  is increased to 0.9. We considered the tonpilz design, and the purpose of the present work was to quantify the design parameters needed to achieve a given  $Q_m$ . The challenges of reaching  $Q_m = 0.6$  or  $Q_m = 0.9$  were compared to those of a more conventional tonpilz design with  $Q_m \approx 2$ . When  $k$  is as high as 0.82, a quality factor of  $Q_m \approx 2$  causes power factor ripple. This ripple was evaluated and the tonpilz response was compared to that of a half-wavelength resonator with matching layers.

### III. ACTIVE MATERIAL

The single crystal material chosen for our calculations was PMN-0.28PT. This material has a very high coupling coefficient in the length extensional mode,  $k_{33} = 0.9$ . The transducers were therefore designed to make the single crystal vibrate in this mode. For the half-wavelength resonator, this can be approached by making a 1-3 composite, with single crystal bars in a matrix of epoxy. With a soft epoxy as kerf filler, the effective coupling coefficient of the composite is close to the single crystal  $k_{33}$ , while a stiffer kerf filler material will reduce the coupling. We considered a plate with 40% PMN-0.28PT in a matrix of the hard-set epoxy Epotek 301-2. The effective coupling for the composite plate was calculated to  $k = 0.82$  using the Smith and Auld model [4]. The effective composite parameters are listed in Table I. The parameters of PMN-0.28PT and Epotek 301-2 are listed in Table II.

In a tonpilz, single crystal bars with the aspect ratio required for length extensional vibration can be supported without using an epoxy matrix. Nevertheless, the effective coupling coefficient of a tonpilz will be reduced by glue and the prestress bolt [3, pp. 169-174]. These effects were not included explicitly in our model, but the effective coupling coefficient resulting from them was estimated to approach 0.8. We therefore chose to use the material parameters of the composite material of Table I also for the active part of the tonpilz model, giving the tonpilz design the same effective coupling coefficient as the plate,  $k = 0.82$ .

### IV. MECHANICAL QUALITY FACTOR OF TONPILZ

To evaluate the achievable  $Q_m$  for a tonpilz, we used the BVD model for a fixed-end, mass-loaded piezoelectric bar, see Fig. 3. The fixed-end can be provided by a large tail-to-head mass ratio. The piezoelectric bar has mass  $M_c$ . When the length  $l$  of the bar is much smaller than a quarter wavelength,  $l \ll \lambda/4$ , the dynamic mass,  $M_d$ , of the bar is  $M_d = \frac{1}{3}M_c$ . We then have [3, p. 159]

$$\omega_0 = \sqrt{\frac{K}{M+M_c/3}} \quad (4)$$

$$Q_m = \omega_0 \frac{M+M_c/3}{R_m} \quad (5)$$

where  $M$  is the mass of the tonpilz head. As the bar is made from the composite material of Table I, the stiffness  $K$  is given by  $K = A_c c_{33}^D / l$ , where  $A_c$  is the area of the composite. Note that the area of single crystal is 40% of  $A_c$ . Assume that the resonance frequency  $\omega_0$  and the tonpilz head area  $A$  are fixed design parameters. Inserting  $K = A_c c_{33}^D / l$  and  $M_c = \rho A_c l$  into (4), we see that for a given  $M$ , there will be a fixed relationship between  $l$  and  $A_c$ . The length  $l$  can therefore be eliminated from the expression for the mass  $M_c$ . The bar area  $A_c$  can be given as a fraction of  $A$ ,  $A_c = A/q_A$ , see Fig. 3. For the case of no loss and real loading,  $R_m$  is proportional to  $A$ . It is then clear from (5) that for a fixed  $M$ ,  $Q_m$  will be given by  $q_A$ . This dependence is illustrated in Fig. 4. The head masses of Fig. 4 are given relative to a reference mass  $M_p$ . The reference mass  $M_p$  was chosen as the mass of a half-wavelength resonator with area  $A$ , made from the material given in Table I. It was introduced to make the illustration independent of resonance frequency.

In Fig. 4,  $Q_m = 0.6$  is reached only for the smallest head mass,  $M = 0.025M_p$ , and only for a large area ratio,  $q_A \gtrsim 10$ , meaning that the area of single crystal is only around 4% of  $A$ . Note that for very small head masses, the length  $l$  of the active bar will not be very small compared to the wavelength. As  $l$  approaches  $\lambda/4$ ,  $M_d$  will approach  $M_c/2$  [3, p. 159]. Reaching the very low values for  $Q_m$  can therefore be even more difficult than illustrated in Fig. 4.

A reduction of  $k$  from 0.9 to 0.82 increases the optimum  $Q_m$  from 0.6 to 0.9. According to Fig. 4, the single crystal area can then be doubled from 4% to 8%. Increasing  $Q_m$  further to 2 while keeping 8% single crystal will allow the head mass  $M$  to be increased by a factor 4. Flexural modes in the head should be placed outside the operating frequency band of the transducer. Increasing  $M$  will increase the frequency of the first

flexural head mode. For a square head, this frequency is given by [3, p. 213]

$$f_f = 1.12 \frac{c_h M}{A^2 \rho_h \sqrt{1-\sigma^2}} \quad (6)$$

where  $c_h$ ,  $\rho_h$  and  $\sigma$  are the speed of sound, the density and the Poisson ratio of the head material. The velocity to density ratio,  $c_h/\rho_h$ , is central in determining  $f_f$ . Fig. 5 shows the ratio required for  $f_f$  to be positioned at twice the resonance frequency. The ratio is calculated for different head masses and head widths,  $\sqrt{A}$ , assuming Poisson ratio  $\sigma = 0.3$ . This  $\sigma$  is an estimate close to the value of most head mass materials. Among the common head materials, magnesium has the highest velocity to density ratio,  $c_h/\rho_h = 2.8 \text{ m}^4/\text{kg/s}$ . Note from Fig. 5 that if  $M$  is as small as  $0.025M_p$ , the width of a square magnesium head must be smaller than  $0.3\lambda$  to avoid flexural modes below  $2\omega_0$ .

TABLE I. EFFECTIVE PARAMETERS OF THE PIEZOCOMPOSITE

Property	Symbol	Units	Piezocomposite
Density	$\rho$	$\text{kg/m}^3$	3930
Velocity	$v^D$	$\text{m/s}$	3612
Dielectric constant	$\epsilon_{33}^S$	$\epsilon_0$	375
Elastic stiffness constant	$c_{33}^D$	$10^{10} \text{ N/m}^2$	5.12
Coupling coefficient	$k$		0.82

TABLE II. MATERIAL PARAMETERS

Property	Symbol	Units	PMN-0.28PT	Epotek 301-2
Elastic stiffness constant	$c_{11}^E$	$10^{10} \text{ N/m}^2$	14.7	0.81
	$c_{12}^E$		13.1	0.46
	$c_{13}^E$		11.4	
	$c_{33}^E$		11.4	
	$c_{44}^E$		6.41	0.17
	$c_{66}^E$		4.02	
Dielectric constant	$\epsilon_{11}^S$	$\epsilon_0$	1605	
	$\epsilon_{33}^S$		885	
	$\epsilon_{33}^T$		4841	
	$e_{31}$		-6.88	
Piezoelectric constant	$e_{33}$	$\text{C/m}^2$	21.4	
	$e_{15}$		11.3	
Piezoelectric constant	$d_{33}$	$10^{-12} \text{ C/N}$	1282	
Density	$\rho$	$\text{kg/m}^3$	8100	1150
Coupling coefficient	$k_{33}$		0.9	

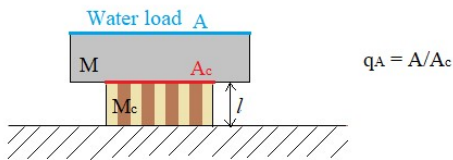


Fig. 3. A fixed-end, mass loaded piezoelectric bar (composite material)

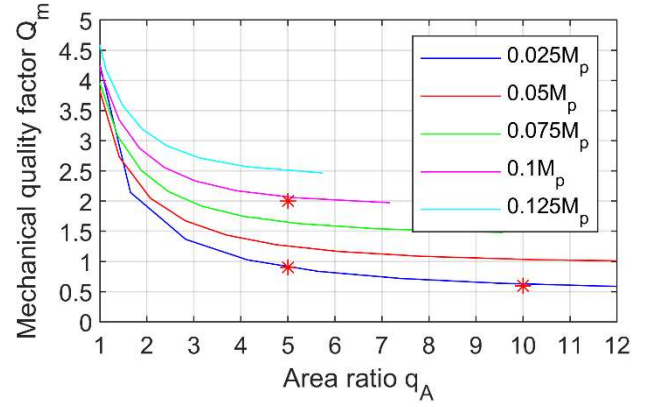


Fig. 4. Mechanical quality factor versus area ratio  $q_A$  for different head masses. Calculated using (5). The masses are given in terms of the reference mass  $M_p$ . Quality factors  $Q_m = 0.6, 0.9$  and  $2$  marked with red dots.

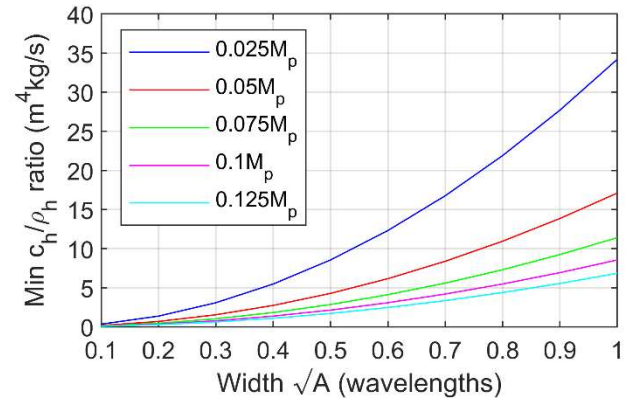


Fig. 5. The  $c_h/\rho_h$  ratio needed for the first flexural mode of a square head to appear at twice the resonance frequency, plotted versus the width of the head. A Poisson ratio of  $\sigma = 0.3$  is assumed.

## V. TONPILZ DESIGN WITH $Q_M \approx 2$ COMPARED TO PLATE WITH MATCHING LAYERS

To achieve the optimum  $Q_m$  of 0.9 for  $k = 0.82$ , the tonpiliz element must have a small head mass. The larger head mass, the smaller amount of active material is allowed, limiting the maximum transmitted power. Flexural resonances due to a small head mass  $M$  can be compensated by a small head area  $A$ , see (6). Decreasing the area of each tonpiliz element will however increase the number of elements needed for a given transducer aperture. We therefore wanted to evaluate the performance of tonpiliz designs with  $Q_m$  larger than the optimum value. The parallel tuned electrical power factor and the normalized acoustic power for a water loaded tonpiliz were evaluated using the 1D Mason model. The distributed Mason model was preferred to the lumped BVD model to get a more correct model for the dynamic mass, and the Mason model was used also for the composite plate with matching layers. The calculated results for a tonpiliz design with  $k = 0.82$  and  $Q_m = 1.9$  are shown in Fig. 6, thick lines. Results using a 3D FEM model with periodic boundary conditions are shown as thin lines, and they are in excellent accordance with the results calculated using the Mason model. The tonpiliz design was made with a square magnesium head with  $M = 0.075M_p$  and

$q_A = 2.7$ . The power factor has pronounced ripple, but it stays above 0.8 in a frequency band that is 150 %, relative to the resonance frequency. The acoustic power varies 10 dB within this band. In Fig. 7 this performance is compared to that of an air-backed composite plate. For the plate design, acoustic matching to water was achieved by adding two matching layers. The matching layer properties were designed for maximum broadband operation, following guidelines given by DeSilets et. al [5]. This matching is frequency dependent, in contrast to the frequency independent matching obtained in a tonpilz. From Fig. 7 we see that compared to the tonpilz, the plate design has larger distance between the  $-3$  dB points of the acoustic power, and very little ripple in the passband, but the acoustic power falls off more rapidly beyond the  $-3$  dB points. This results in larger power factor ripple outside the passband. It should be noted that in Fig. 7 the power factor ripple for the plate design is minimized by making a small adjustment of the tuning frequency. The chosen tuning frequency is 6 % lower than the resonance frequency of the plate. The matching layers were designed inserting the short circuit acoustic impedance of the plate into DeSilets' expressions, rather than the default open circuit impedance. This did also contribute to a reduction of the power factor ripple.

## VI. DISCUSSION

When the aim is to provide narrowband pulses at a variety of frequencies, rather than one wideband pulse spanning the entire band, the tonpilz has the preferred performance of the two designs in Fig. 7.

A clamped back end or high attenuation in the backing or matching layers would reduce the power factor ripple of the plate design. Attenuation is not included in the modelled matching layers. On the other hand, disturbance from the first flexural resonance of the tonpilz head could be prevented by distributing the crystal bars as done in Powers et. al [6], or by tapering the heads. This would allow a lighter head and thus a smaller  $Q_m$ , reducing the power factor ripple of the tonpilz design. The curves of Fig. 5 are calculated for square heads. For circular heads, the frequency of the first flexural mode is higher than for square heads [3, p. 213], but square heads were chosen as they provide an array packing factor close to 1 and thus a large radiation resistance.

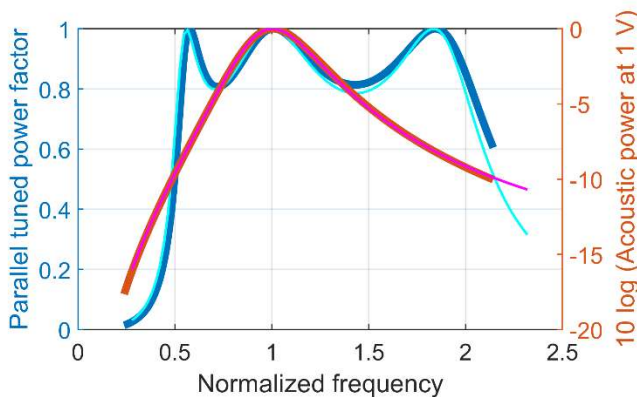


Fig. 6. Parallel tuned electrical power factor (blue) and normalized acoustic power (red) for a tonpilz design with  $k = 0.82$  and  $Q_m = 1.9$ . Thick lines: 1D Mason model. Thin lines: 3D FEM model with periodic boundary conditions.

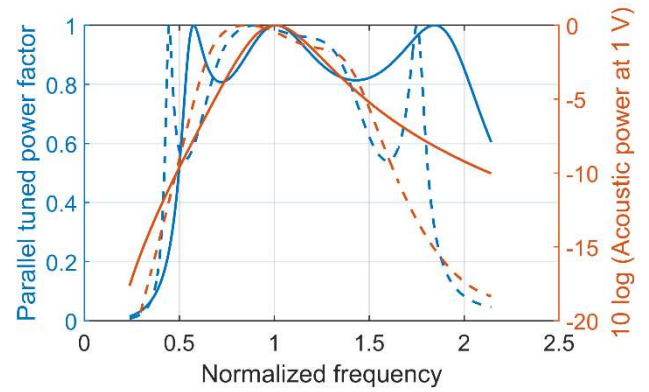


Fig. 7. Parallel tuned electrical power factor (blue) and normalized acoustic power (red). Comparison of a tonpilz design with  $k = 0.82$  and  $Q_m = 1.9$  (solid lines) and a design comprised of a composite plate (also  $k = 0.82$ ) and two added matching layers (dashed lines).

## VII. CONCLUSIONS

We compared two different transducer designs, using an active material with very high electromechanical coupling to obtain a transmitter with a large usable band. The transducers were designed for applications where the amount of reactive power constitutes a main restriction and where the aim is to offer a selection of narrowband pulses at a variety of frequencies rather than one wideband pulse. Under these considerations, we found that the tonpilz design performed better than a design consisting of an air-backed composite plate and two matching layers. The effective coupling coefficient of our designs was  $k = 0.82$ , and the optimum mechanical quality factor for this  $k$  is  $Q_m \approx 0.9$ . This  $Q_m$  can be difficult to obtain in a practical design. We found that even for  $Q_m \approx 2$  the tonpilz design performed better than the composite plate design, under the given considerations. For the plate design, the frequency dependence of the matching layers caused the acoustic power to fall off rapidly beyond the  $-3$  dB points, resulting in large ripple in the electrical power factor.

## REFERENCES

- [1] D. Stansfield, "Bandwidth" in Underwater Electroacoustic Transducers, 1<sup>st</sup> ed., Bath, UK: Bath University Press, 1991, ch. 5, sec. 3, pp. 112-119
- [2] M. B. Moffett, H. C. Robinson, J. M. Powers, and P. D. Baird, "Single-crystal lead magnesium niobate-lead titanate (PMN/PT) as a broadband high power transduction material", J. Acoust. Soc. Am, vol. 121, no.5, pp. 2591-2599, May 2007.
- [3] C. H. Sherman and J. L. Butler, Transducers and Arrays for Underwater Sound, 2<sup>nd</sup> ed., Cham, Switzerland: Springer International Publishing, 2016.
- [4] W. A. Smith and B. A. Auld, "Modeling 1-3 composite piezoelectrics: Thickness-mode oscillations," IEEE Trans. Ultrason., Ferroelect., Freq. Contr., vol. 38, no. 1, pp. 40-47, 1991.
- [5] C. S. DeSilets, J. D. Fraser and G. S. Kino, "The design of efficient broadband piezoelectric transducers", IEEE Trans. Son. Ultrason., Vol. 25, no. 3, pp. 115-125, May 1978.
- [6] J. M. Powers, M. B. Moffett, and F. Nussbaum, "Single crystal naval transducer development", IEEE Int. Symp. Appl. Ferroelect., Honolulu, US (HI), 2000, pp. 351-354